



A Journal of the Gesellschaft Deutscher Chemiker

Angewandte Chemie

GDCh

International Edition

www.angewandte.org

Accepted Article

Title: Exploring the “Goldilocks Zone” of Semiconducting Polymer Photocatalysts via Donor-Acceptor Interactions

Authors: Yaroslav S. Kochergin, Dana Schwarz, Amitava Acharjya, Arun Ichangi, Ranjit Kulkarni, Pavla Eliášová, Jaroslav Vacek, Johannes Schmidt, Arne Thomas, and Michael Janus Bojdys

This manuscript has been accepted after peer review and appears as an Accepted Article online prior to editing, proofing, and formal publication of the final Version of Record (VoR). This work is currently citable by using the Digital Object Identifier (DOI) given below. The VoR will be published online in Early View as soon as possible and may be different to this Accepted Article as a result of editing. Readers should obtain the VoR from the journal website shown below when it is published to ensure accuracy of information. The authors are responsible for the content of this Accepted Article.

To be cited as: *Angew. Chem. Int. Ed.* 10.1002/anie.201809702
Angew. Chem. 10.1002/ange.201809702

Link to VoR: <http://dx.doi.org/10.1002/anie.201809702>
<http://dx.doi.org/10.1002/ange.201809702>

COMMUNICATION

Exploring the “Goldilocks Zone” of Semiconducting Polymer Photocatalysts *via* Donor-Acceptor Interactions

Yaroslav S. Kochergin,^[a, b] Dana Schwarz,^[b] Amitava Acharjya,^[c] Arun Ichangi,^[a] Ranjit Kulkarni,^[a, e] Pavla Eliášová,^[d] Jaroslav Vacek,^[a] Johannes Schmidt,^[c] Arne Thomas^[c] and Michael J. Bojdys*^[a, e]

Abstract: Water splitting using polymer photocatalysts is a key technology to a truly sustainable hydrogen-based energy economy. Synthetic chemists have intuitively tried to enhance photocatalytic activity by tuning the length of π -conjugated domains of their semiconducting polymers, but the increasing flexibility and hydrophobicity of ever-larger organic building blocks leads to adverse effects such as structural collapse and inaccessible catalytic sites. To reach the ideal optical bandgap of ~ 2.3 eV, we synthesised a library of eight sulphur and nitrogen containing porous polymers (SNPs) with similar geometries but with optical bandgaps ranging from 2.07 to 2.60 eV using Stille coupling. These polymers combine π -conjugated electron-withdrawing triazine- (C_3N_3) and electron donating, sulphur-containing moieties as covalently-bonded donor-acceptor frameworks with permanent porosity. The remarkable optical properties of SNPs enable fluorescence on-off sensing of volatile organic compounds and illustrate intrinsic charge-transfer effects. Moreover, obtained polymers effectively evolve H_2 gas from water under visible light irradiation with hydrogen evolution rates up to $3158 \mu\text{mol h}^{-1} \text{g}^{-1}$ and high apparent quantum efficiency which is the highest value obtained for microporous organic polymers to-date. The design principles demonstrated here are transferable to a new field of high-performance polymer photocatalysts based on efficient donor-acceptor dyads.

The bandgap is arguably the most critical parameter in the design of semiconducting polymer materials with end-applications in photocatalysis, sensing, solar cells, and solid-state light emission.^[1] In photocatalytic water splitting, the ideal bandgap has to straddle the proton reduction and the water oxidation potentials. In practice, only one half-reaction – proton reduction – occurs preferentially, because the four-hole water oxidation is sluggish in comparison to spontaneous electron-hole

recombination within the catalyst.^[2] Sacrificial electron donors, such as triethanolamine (TEOA), that have more negative potentials and require only two-hole oxidation are routinely employed and experiments show that this changes the optimal bandgap to 2.2 to 2.4 eV.^[3] Synthetic strategies to narrow-down the optical bandgap of polymers commonly rely on sequential increases of the size of π -conjugated segments and hence, a red-shift of the optical adsorption edge.^[4] For example, conjugated microporous polymers (CMPs) are based on polycyclic, aromatic hydrocarbons of varying lengths,^[5] and they have found applications in organic electronics as light emitters,^[3a] polymer light emitting diodes (PLEDs) and solar cells,^[6] and as photocatalysts.^[7] The disadvantage of this design strategy is that (1) the ever-increasing size of organic tectons introduces more flexibility into the polymer network, shortens the effective π -conjugation length and ultimately causes pore collapse, and (2) a majority of large organic tectons are apolar leading to low wettability in water, and hence low water splitting efficiency.

An alternative approach employs donor-acceptor (D-A) dyads for bandgap tuning. For example, a photoactive triazine-containing D-A polymer was successfully used for photocatalytic conversion of organic molecules.^[8] Moreover, D-A dyads with sulphur-containing donor groups and electronegative (nitrogen- and oxygen-containing) acceptor groups enable very narrow bandgaps,^[9] tuning of emitted colour,^[10] and enhanced photoluminescence.^[11] In the context of polymer photocatalysts, D-A motifs remain largely unexplored with very few recent examples such as heptazine-based polymer networks (HMPs),^[12] and sulphur- and nitrogen-containing porous polymers (SNPs)^[3b] that achieve comparatively low hydrogen evolution rates of $32 \mu\text{mol h}^{-1} \text{g}^{-1}$ (for HMP-3) and $452 \mu\text{mol h}^{-1} \text{g}^{-1}$ (for SNP-2). Calculations suggest that D-A systems have narrow bandgaps only if there are weak D-A interactions, while strong interactions lead to charge-transfer and wide bandgaps.^[13] Incorporating D-A motifs into polymer photocatalysts is still useful, since fast electron-hole recombination is a major detrimental factor for efficient photocatalysis.^[1-2] We explore D-A polymer photocatalysts in a systematic fashion in order to identify the “Goldilocks Zone” in which the bandgap is sufficiently wide to enable proton reduction, and where charge-transfer is sufficiently strong to prevent undesired electron-hole recombination. To this end, we combine C_2 and C_3 symmetric building blocks of similar sizes that contain electron-rich sulphur-moieties and electron-withdrawing triazine (C_3N_3) units (Scheme 1). Aryl spacers are introduced around the electron-withdrawing triazine-moiety to test the effect of weak D-A interactions on charge-transfer in a simple photoluminescence excitation (PLE) study using volatile organic compounds (VOCs).^[13a] Having identified the trend, that charge-transfer fluorescence is enhanced in strongly interacting D-A polymers, we proceed to select the systems closest to a ~ 2.3 eV bandgap – the “Goldilocks Zone” – and test their activities in photocatalytic water splitting. Remarkably, we identify three (out of eight) polymer systems with some of the highest hitherto reported hydrogen evolution rates for as-received catalysts of

[a] Y. S. Kochergin, A. Ichangi, Ranjit Kulkarni, Dr. J. Vacek, Dr. M. J. Bojdys

Institute of Organic Chemistry and Biochemistry of the CAS
Flemingovo nám. 2, 166 10 Prague, Czech Republic
E-mail: m.j.bojdys.02@cantab.net

[b] Y. S. Kochergin, Dr. D. Schwarz
Department of Organic Chemistry
Charles University in Prague

Hlavova 8, 128 00 Prague, Czech Republic

[c] A. Acharjya, Dr. J. Schmidt, Prof. Dr. A. Thomas
Institute of Chemistry

Technische Universität Berlin
Hardenbergstraße 40, 10623 Berlin, Germany

[d] Dr. P. Eliášová
Department of Physical and Macromolecular Chemistry
Charles University in Prague

Hlavova 8, 128 00 Prague, Czech Republic

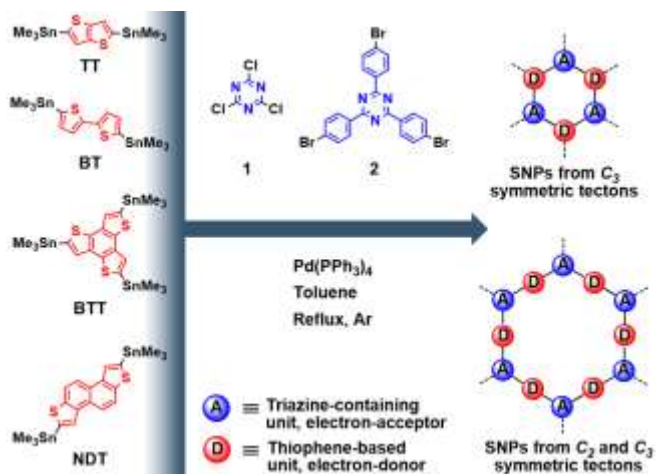
[e] R. Kulkarni, Dr. M. J. Bojdys
Department of Chemistry

Humboldt-Universität zu Berlin
Brook-Taylor-Str. 2, 12489 Berlin, Germany

Supporting information for this article is given via a link at the end of the document.

COMMUNICATION

between 2627 and 3158 $\mu\text{mol h}^{-1} \text{g}^{-1}$ at apparent quantum efficiencies of up to 4.5%. To our knowledge, these values have been exceeded only by one photocatalytic system, a poly(triazine imide) which was post-synthetically modified with 4-amino-2,6-dihydropyrimidine (aPTI_4AP_{16%}) that reached 4907 $\mu\text{mol h}^{-1} \text{g}^{-1}$ at a lower quantum efficiency of 3.4%.^[14]



Scheme 1. Synthetic pathway toward sulphur and nitrogen containing porous polymers (SNPs). C_2 and C_3 symmetric thiophene-based electron-acceptors (in red) are coupled with C_3 symmetric triazine-containing electron acceptors (in blue).

We chose four thiophene-containing tectons as electron donors: thienothiophene (TT), bithiophene (BT), benzotrithiophene (BTT), and naphthodithiophene (NDT). Their stannylated derivatives are coupled with commercially available cyanuric chloride (1) and easy-to-synthesise tri-bromophenyltriazine (2) via Pd-catalysed Stille coupling (Scheme 1). The synthetic protocols for all tectons and polymers can be found in the Supporting Information section (Table S1 and S2). In total, eight new SNPs were prepared in excellent yields (Table 1 and S2). Chemical environments were identified by ^{13}C cross-polarization magic-angle spinning (CP-MAS) NMR spectroscopy (Figure 1). All SNPs show the characteristic triazine-ring carbon signal in the region between 169-172 ppm. Signals in the range from 110 to 150 ppm are assigned to sp^2 -hybridised carbon atoms within aryl spacers and thiophene moieties. The triazine breathing mode is visible in Fourier-transform infrared (FT-IR) spectra (Figure S33) as a sharp signal around 820-810 cm^{-1} .^[15] Elemental composition was determined by combustion elemental analysis (EA), inductively coupled plasma optical emission spectrometry (ICP-OES), energy dispersive X-ray spectroscopy (EDX), X-ray photoelectron spectroscopy (XPS) and thermogravimetric analysis (TGA) under air and matched the expected values (Table S3, S4, and S7-S14, Figure S2 and Figure S43-S50). According to ICP-OES, traces of palladium that stem from the coupling reaction of 0.07-1.53 wt% are present in all synthesised SNPs as inclusions inside the polymer matrix. Additional unreacted end groups show Cl and Br (0-3.26 wt%) along with Sn (0-0.85 wt%) in non-stoichiometric amounts.

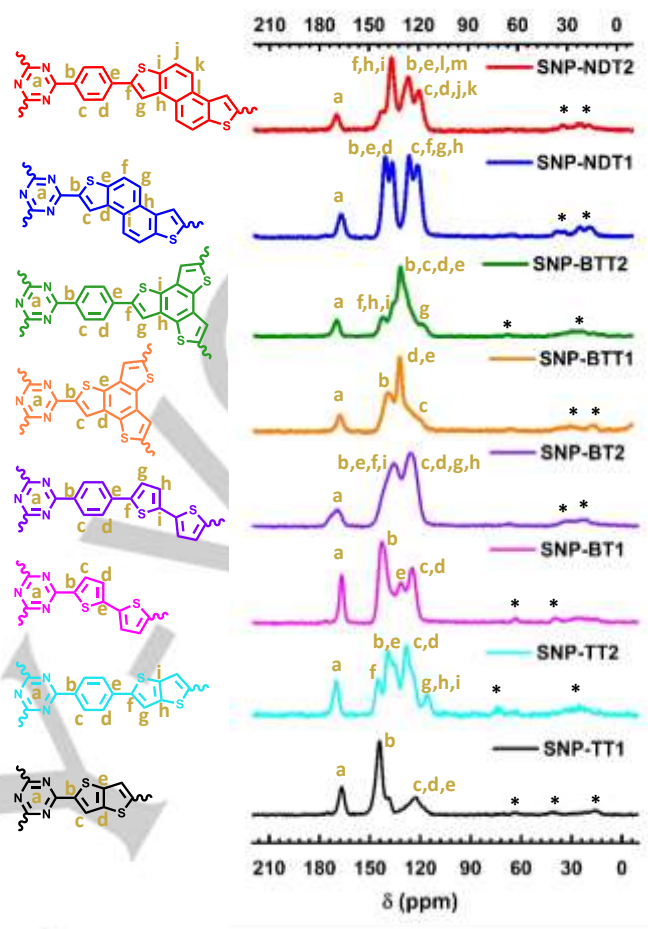


Figure 1. ^{13}C cross-polarization magic angle spinning solid-state NMR spectra of SNPs. Triazine carbons appear at 170 ppm. Signals between 110 and 150 ppm correspond to phenyl and thiophene carbon atoms. Spinning side bands are marked with an asterisk (*).

Powder X-ray diffraction (PXRD) shows that all SNPs are predominantly amorphous with some degree of preferred ordering in the low-angle region between 5 and 20° 2 θ (Figure S27). This is typical for conjugated polymers synthesised via transition-metal catalysed reactions, such as Stille coupling,^[16] due to the irreversible formation of carbon-carbon bonds and kinetic reaction control. Interlayer stacking peaks around 25° 2 θ for **SNP-TT1**, **SNP-BT1**, **SNP-BTT1** and **SNP-NDT1** are also observed in other layered, aromatic systems such as CMPs and covalent organic frameworks (COFs).^[17] Tris-phenyltriazine-based analogues **SNP-TT2**, **SNP-BT2**, **SNP-BTT2** and **SNP-NDT2** do not show peaks in this region, presumably because of higher flexibility around the aryl spacer (Figures S36-S43). Electron microscopy images of all SNPs show “cauliflower”-shaped aggregates typical for kinetically controlled nucleation growth (Figure S11 – S28). High-resolution images, however, reveal pronounced moiré

COMMUNICATION

fringes as well as visible concentric rings in selected-area electron-diffraction (SAED) patterns. These rings correspond to regular distances within the principal unit-cells and indicate that these SNPs feature polycrystalline domains.^[18]

We studied the guest-accessible pore-space of all polymers by nitrogen (N_2) adsorption/desorption (Figure S28a). All materials show Type I adsorption isotherms indicating the presence of micropores.^[19] The accessible Brunauer–Emmett–Teller (BET) surface areas are in the range from 53 to 698 $m^2 g^{-1}$ (Table 1). Polymers containing a freely-rotating aryl spacer have on average smaller surface areas compared to their directly coupled analogues. The pore size distribution (PSD) was analysed for the materials with highest surface areas (Figure S28b), and it shows pore sizes between 1 and 2 nm in the micropore region. We achieve comparable surface polarities for all synthesised SNPs, and enhanced CO_2 physisorption as a consequence of the high heteroatom loading (Figure S29).^[3b, 20] Prepared SNPs have a moderate reversible CO_2 uptake between 0.69 to 2.04 $mmol g^{-1}$ at 273 K (Figure S29c); comparable to the hitherto reported values for CMPs.^[21]

Solid-state diffuse-reflectance UV-vis measurements show a range of discernible adsorption edges starting at 470 nm for **SNP-BTT2** to 600 nm for **SNP-BT1** (Figure 2a). According to the Kubelka-Munk equation these values correspond to direct optical bandgaps between 2.07 and 2.60 eV and indirect bandgaps between 1.71 and 2.38 eV (Figure S30). As a general trend, polymers that contain an aryl spacer also have a larger optical bandgap compared to their directly coupled analogues, except for the naphthodithiophene- (NDT) based network (Table 1). These results seem to contradict theoretical predictions that strong D-A interactions would widen the bandgap,^[13a] and they highlight the continuous problems of DFT with respect to complex, organic D-A systems. All materials have pronounced fluorescence in solid-state photoluminescence emission (PLE) measurements that does not stem from their molecular building blocks (Figure S32). We observe a range of PLE maxima from 542 nm (1.96 eV) for **SNP-BT1** to 630 nm (2.30 eV) for **SNP-NDT1** (Figure 2b), i.e. from light-blue to dark-red (Figure 2c). These PL transitions correlate best with indirect bandgaps obtained from UV-vis spectra (Table 1). DFT calculations (PBE and PBE0) confirm that – in general – the lowest-energy transitions in all SNPs correspond to indirect bandgaps (Table S6). Hence, we conclude that all SNPs are indirect bandgap semiconductors.

The strong fluorescence of all SNPs yields itself to sensing of volatile organic compounds (VOCs) with different polarities: chlorobenzene, xylene, toluene, benzene, nitrobenzene, and benzonitrile (Figure S59). PLE intensity increased significantly upon adsorption of electron-rich aromatic VOCs like benzene. In these instances, the LUMO of electron-rich arenes is energetically higher than the well of the SNP conduction band, and hence, additional electrons are driven into the polymer. Conversely, exposure to vapours of electron-deficient arenes such as nitrobenzene leads to fluorescence quenching as excited electrons are being depleted (Figure S60).^[22] The position of absorption maxima of individual SNPs did not change significantly upon VOC adsorption, indicating that the electronic structure of the ground state remained unchanged, and hence, pointing towards (weak) physisorption of VOCs.^[23] Most noteworthy, the changes in fluorescence are systematically lower for SNPs with

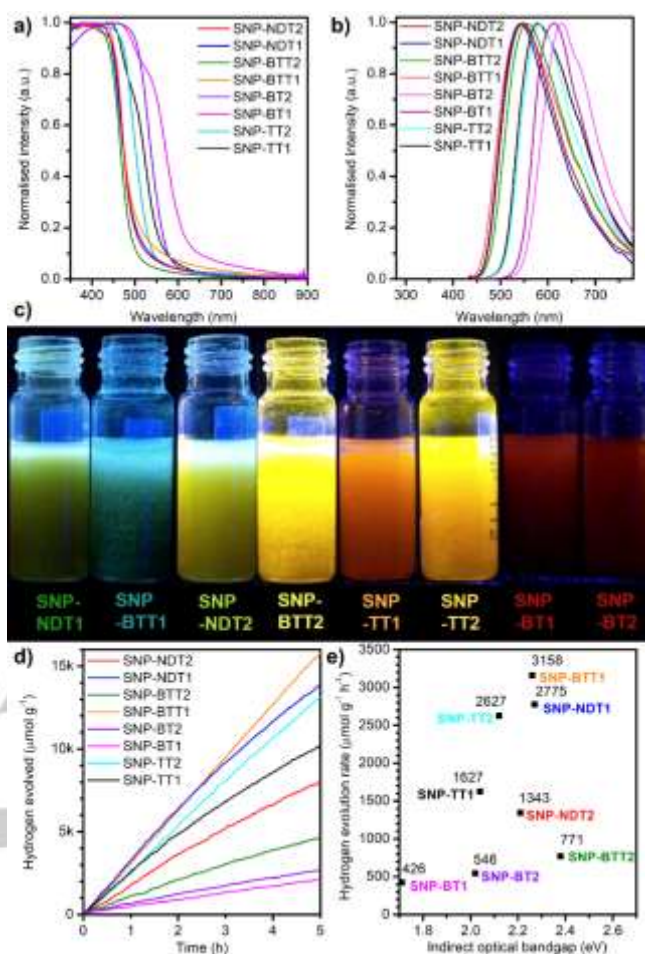


Figure 2. a) Normalised solid-state UV-vis diffuse-reflectance spectra; b) Normalised solid-state photoluminescence emission spectra ($\lambda_{excit} = 400$ nm); c) Photographs of polymers under irradiation with UV light ($\lambda_{excit} = 365$ nm) in benzene (3 $mg mL^{-1}$); d) Hydrogen evolution rates (HER) of SNPs during 5 h experiments performed under visible light (395 nm cut-off filter) in a water/acetonitrile (1:1) mixture using triethanolamine (TEOA) as sacrificial agent and 3 wt% platinum as a co-catalyst; e) Correlation of HER with the indirect optical bandgaps of prepared SNPs.

an aryl spacer between the D-A moieties (all **SNPs-2**), and higher for those without (all **SNPs-1**) (Figure S61). The relative changes of fluorescence are independent of guest-accessible surface area. Hence, it is not the number of adsorbed VOCs that influences fluorescence, but the relative positions of the conduction bands of the SNPs.

We attempt to qualitatively assess this charge-transfer effect *via* DFT calculations of the LUMO and HOMO of suitable cluster models. Plots of the LUMO/HOMO isosurfaces (calculated with G16@B3LYP/cc-pVDZ/GD3, Figure S42) indicate that the LUMOs of all SNP-1 systems have more defined, localized lobes positioned on the heteroatoms of the D-A moieties. LUMOs of all **SNP-2** systems plotted at identical scaling factors are more delocalised, presumably because of partial charge-transfer into the aryl spacer. The PLE study and DFT calculations indicate that directly coupled D-A moieties experience stronger charge-transfer than D-A moieties that are held apart by an aryl linker.

COMMUNICATION

Therefore, we can expect better electron-hole separation in SNP-1 systems, and hence, a more efficient photocatalysis.

Table 1. Porous and optical properties of SNPs.

Network	S _{BET} (m ² g ⁻¹) ^[a]	CO ₂ uptake (mmol g ⁻¹) ^[b]	E _{g,direct} (eV) ^[c]	E _{g,indirect} (eV) ^[d]	E _{PL} (eV) ^[e]
SNP-TT1	443	1.76	2.28	2.04	2.15
SNP-TT2	384	0.69	2.42	2.12	2.11
SNP-BT1	53	0.97	2.07	1.71	1.96
SNP-BT2	94	0.82	2.27	2.02	2.02
SNP-BTT1	698	2.03	2.57	2.26	2.28
SNP-BTT2	411	1.38	2.60	2.38	2.22
SNP-NDT1	656	2.04	2.56	2.27	2.30
SNP-NDT2	79	0.86	2.50	2.21	2.26

[a] Surface area calculated from N₂ adsorption isotherm using BET equation; [b] CO₂ uptake calculated at 273 K and 1 bar; [c] Direct and [d] indirect optical bandgaps calculated *via* the Kubelka-Munk function; [e] Maximum of photoluminescence emission measured in solid state.

We have seen so far that all SNPs have a suitably situated, indirect bandgap between 1.71 and 2.38 eV, and that the sub-set of SNPs that contains directly coupled D-A moieties (all SNP-1 systems) will presumably be able to separate electrons and holes better due to stronger charge-transfer effects. Moreover, structural polarity due to high heteroatom content, and rigidity of monomeric building units will improve, in general, the wettability of obtained polymers in aqueous solution (Figure S63). We put this knowledge to the test and examine all materials with respect to their activity in photocatalytic hydrogen evolution from water using platinum (Pt) co-catalyst and triethanolamine (TEOA) as sacrificial agent. All prepared SNPs show stable hydrogen production under visible light (395 nm cut-off filter) for at least 5 h (Figure 2d). Long-term measurement for 50 h of the best-performing **SNP-BTT1** network shows a stable increase in hydrogen gas evolved (Figure S64a) with a hydrogen evolution rate (HER) of 3158 μmol h⁻¹ g⁻¹, which is, the highest reported value for as-received, amorphous CMPs and one of the highest among microporous organic polymers (Table S17). Apparent quantum efficiency (AQE) was measured as a function of incident light using bandpass filters with a central wavelength of 420 nm and totalled to an excellent 4.5% (Figure S67). Even without additional co-catalyst **SNP-BTT1** shows an excellent HER of 489 μmol h⁻¹ g⁻¹ (Figure S64b).

Since all materials were obtained *via* Pd-catalysed Stille coupling, it is possible, that residual Pd content may facilitate the proton reduction on SNPs, acting as an additional metal co-catalyst. There are several studies that show that there is no clear correlation between residual Pd-catalyst from the cross-coupling reaction and photocatalytic activity, since the contribution of 3 wt% Pt co-catalyst outweighs any contribution from Pd.^[4b, 24] This is also the case in the present work (Figure S66). **SNP-TT1** polymer with Pt co-catalyst has the largest Pd-content of 1.53 wt%, yet it only shows moderate HER of 1627 μmol h⁻¹ g⁻¹,

whereas only 0.61 wt% of Pd was found in the **SNP-BTT1** network which has the highest hydrogen evolution activity. In addition, we performed a control experiment without any polymer, adding only H₂PtCl₆, which is used as the Pt source in conventional hydrogen evolution experiments. As a result, no H₂ was evolved, confirming, that metals on their own cannot facilitate hydrogen gas production. Exchange of Pt co-catalyst to Pd can even diminish photocatalytic activity of conjugated porous polymers, as it was shown in our previous study.^[25]

In summary, we set out to examine rational design-concepts for enhanced photocatalysts based on the highly-modular family of sulphur and nitrogen containing porous polymers (SNPs). We designed eight SNP systems that feature a similar pore structure yet have a range of optical bandgaps and come with and without spacers between the donor- (aromatic thiophenes) and acceptor- (triazine) moieties to enable strong and weak charge-transfer effects, respectively. Composition, properties and computational rationalization of these polymers narrows down the "Goldilocks Zone" for the ideal polymer photocatalyst as follows: (1) There is a conceivable range of optimal (indirect) bandgaps for photocatalysis between 2.1 and 2.3 eV that eclipses the proton reduction and the sacrificial donor oxidation potentials. This zone can be reached without ever-expanding sizes of π-aromatic synthons that compromise wettability and structural stability of networks, but rather with push-pull effects induced by donor-acceptor interactions. (2) Efficient charge-separation is key in preventing inefficient, spontaneous electron-hole recombination, and it can be achieved by strong D-A interactions and short pathways between donor and acceptor moieties. Here, on/off fluorescence screening by adsorption of volatile organic compounds may be a viable tool to test the strength of charge-transfer and to easily screen for suitable materials.

The photocatalysts designed on these two concepts have an outstanding performance with one of the highest hydrogen evolution rates of 3158 μmol h⁻¹ g⁻¹ – 1.6 times higher than any previously reported value for as-received polymer photocatalysts – with an excellent apparent quantum yields of 4.5%. These findings cement the importance of donor-acceptor dyads for efficient charge-separation, and they challenge the common misconception that strong charge-transfer is detrimental in the bandgap-engineering of semiconductor photocatalyst. Ultimately, the versatile, mix-and-match synthetic platform presented here may yet hold the key for the design of photo- and electro-active (semi-)conducting polymer materials for light-driven catalysis – where charge separation become important – and in electronic application – where aromatic spacers enable enhanced charge-carrier mobility.

Experimental Section

General procedure for Stille-coupling polymerisation.

Overview of all prepared materials could be find in Table S1.

Stannylated thiophene-based derivative, triazine-containing monomer and Pd(PPh₃)₄ (3:2:5% molar ratio; in case of benzo[1,2-b:3,4-b':5,6-b'']trithiophene (**3a**) – 1:1:5% molar ratio) were dissolved in anhydrous

COMMUNICATION

toluene under inert atmosphere and refluxed for 3 days. In a short time period (1-2 h) the precipitate of polymer started to appear in the reaction flask. After completion of the reaction the precipitate was filtered and washed with hot toluene, DMF, chloroform, THF and methanol (3 times each solvent). Subsequently the Soxhlet extraction was performed using chloroform, THF and methanol (24 h each solvent). Afterwards the solid was dried in the vacuum drying oven at 120 °C for 24 h. More detailed reaction parameters can be found in Table S2.

Acknowledgements

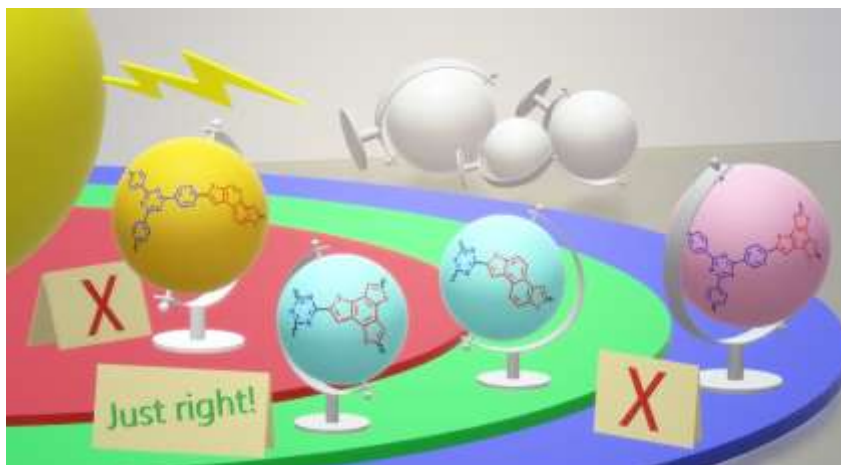
We thank Mária Piatková, Martina Rimmel and André Sanches for upscaling and help with fluorescence measurements, Barbora Balcarova for N₂ sorption measurements, Stanislava Matějková for ICP-OES, Adam Málek for IR spectroscopy measurements, Martin Dračinský for access to solid-state NMR facilities, and Dr. Miroslav Štěpánek for solid-state fluorescence measurements. A.A., J.S. and A.T. acknowledge support from the German Science Foundation (Project TH1463/15-1) and the Cluster of Excellence (UniCat). M.J.B. thanks the European Research Council (ERC) for funding under the Starting Grant Scheme (BEGMAT-678462).

Keywords: conjugated microporous polymers • donor-acceptor systems • fluorescence sensing • photocatalysis • triazine

- [1] F. K. Kessler, Y. Zheng, D. Schwarz, C. Merschjann, W. Schnick, X. Wang, M. J. Bojdys, *Nat. Rev. Mat.* **2017**, *2*, 17030.
- [2] P. Guiglion, C. Butchosa, M. A. Zwijnenburg, *Macromol. Chem. Phys.* **2016**, *217*, 344-353.
- [3] a) J.-X. Jiang, A. Trewin, D. J. Adams, A. I. Cooper, *Chem. Sci.* **2011**, *2*, 1777-1781; b) D. Schwarz, Y. S. Kochergin, A. Acharjya, A. Ichangi, M. V. Opanasenko, J. Čejka, U. Lappan, P. Arki, J. He, J. Schmidt, P. Nachtigall, A. Thomas, J. Tarábek, M. J. Bojdys, *Chem. - Eur. J.* **2017**, *23*, 13023-13027.
- [4] a) J. Roncali, *Macromol. Rapid Commun.* **2007**, *28*, 1761-1775; b) R. S. Sprick, J.-X. Jiang, B. Bonillo, S. Ren, T. Ratvijitvech, P. Guiglion, M. A. Zwijnenburg, D. J. Adams, A. I. Cooper, *J. Am. Chem. Soc.* **2015**, *137*, 3265-3270.
- [5] J.-X. Jiang, F. Su, A. Trewin, C. D. Wood, N. L. Campbell, H. Niu, C. Dickinson, A. Y. Ganin, M. J. Rosseinsky, Y. Z. Khimyak, A. I. Cooper, *Angew. Chem. Int. Ed.* **2007**, *46*, 8574-8578.
- [6] C. Gu, Y. Chen, Z. Zhang, S. Xue, S. Sun, K. Zhang, C. Zhong, H. Zhang, Y. Pan, Y. Lv, Y. Yang, F. Li, S. Zhang, F. Huang, Y. Ma, *Adv. Mater.* **2013**, *25*, 3443-3448.
- [7] R. S. Sprick, B. Bonillo, M. Sachs, R. Clowes, J. R. Durrant, D. J. Adams, A. I. Cooper, *Chem. Commun.* **2016**, *52*, 10008-10011.
- [8] W. Huang, J. Byun, I. Rörich, C. Ramanan, P. W. M. Blom, H. Lu, D. Wang, L. C. d. Silva, R. Li, LeiWang, K. Landfester, K. A. I. Zhang, *Angew. Chem. Int. Ed.* **2018**, *57*, 8316-8320.
- [9] E. E. Havinga, W. ten Hoeve, H. Wynberg, *Polymer Bulletin* **1992**, *29*, 119-126; b) C. R. Chenthamarakshan, J. Eldo, A. Ajayaghosh, *Macromolecules* **1999**, *32*, 251-257.
- [10] a) M. Belletête, J.-F. Morin, S. Beaupré, M. Ranger, M. Leclerc, G. Durocher, *Macromolecules* **2001**, *34*, 2288-2297; b) S. A. Jenekhe, L. Lu, M. M. Alam, *Macromolecules* **2001**, *34*, 7315-7324.
- [11] a) M. Held, Y. Zakharko, M. Wang, F. Jakubka, F. Gannott, J. W. Rumer, R. S. Ashraf, I. McCulloch, J. Zaumseil, *Org. Electron.* **2016**, *32*, 220-227; b) A. Facchetti, *Mater. Today* **2013**, *16*, 123-132.
- [12] K. Kailasam, M. B. Mesch, L. Möhlmann, M. Baar, S. Blechert, M. Schwarze, M. Schröder, R. Schomäcker, J. Senker, A. Thomas, *Energy Technol.* **2016**, *4*, 744-750.
- [13] a) U. Salzner, *J. Phys. Chem. B* **2002**, *106*, 9214-9220; b) M. Keshtov, D. Godovsky, V. Kochurov, G. D. Sharma, F.-C. Chen, N. Radychev, A. Khokhlov, *AIP Conference Proceedings* **2014**, *1599*, 498-501.
- [14] K. Schwinghammer, B. Tuffy, M. B. Mesch, E. Wirnhier, C. Martineau, F. Taulelle, W. Schnick, J. Senker, B. V. Lotsch, *Angew. Chem. Int. Ed.* **2013**, *52*, 2435-2439.
- [15] a) D. Schwarz, Y. Noda, J. Klouda, K. Schwarzová-Pecková, J. Tarábek, J. Rybáček, J. Janoušek, F. Simon, M. V. Opanasenko, J. Čejka, A. Acharjya, J. Schmidt, S. Selve, V. Reiter-Scherer, N. Severin, J. P. Rabe, P. Ecorchard, J. He, M. Polozij, P. Nachtigall, M. J. Bojdys, *Adv. Mater.* **2017**, *29*, 1703399-n/a; b) S. Kuecken, A. Acharjya, L. Zhi, M. Schwarze, R. Schomacker, A. Thomas, *Chem. Commun.* **2017**, *53*, 5854-5857.
- [16] M.-S. Kim, C. S. Phang, Y. K. Jeong, J. K. Park, *Polym. Chem.* **2017**, *8*, 5655-5659.
- [17] P. Kuhn, M. Antonietti, A. Thomas, *Angew. Chem. Int. Ed.* **2008**, *47*, 3450-3453.
- [18] M. Valamanesh, C. Langlois, D. Alloyeau, E. Lacaze, C. Ricolleau, *Ultramicroscopy* **2011**, *111*, 149-154.
- [19] K. S. W. Sing, D. H. Everett, R. A. W. Haul, L. Moscou, R. A. Pierotti, J. Rouquerol, T. Siemienińska, *Pure Appl. Chem.* **1985**, *57*, 603-619.
- [20] S. Ren, M. J. Bojdys, R. Dawson, A. Laybourn, Y. Z. Khimyak, D. J. Adams, A. I. Cooper, *Adv. Mater.* **2012**, *24*, 2357-2361.
- [21] a) S. Ren, R. Dawson, D. J. Adams, A. I. Cooper, *Polym. Chem.* **2013**, *4*, 5585-5590; b) H. Bohra, S. Y. Tan, J. Shao, C. Yang, A. Efrem, Y. Zhao, M. Wang, *Polym. Chem.* **2016**, *7*, 6413-6421; c) Y. Liao, J. Weber, B. M. Mills, Z. Ren, C. F. J. Faul, *Macromolecules* **2016**, *49*, 6322-6333.
- [22] a) X. Liu, Y. Xu, D. Jiang, *J. Am. Chem. Soc.* **2012**, *134*, 8738-8741; b) S. Gu, J. Guo, Q. Huang, J. He, Y. Fu, G. Kuang, C. Pan, G. Yu, *Macromolecules* **2017**, *50*, 8512-8520.
- [23] J.-K. Chen, S.-M. Yang, B.-H. Li, C.-H. Lin, S. Lee, *Langmuir* **2018**, *34*, 1441-1446.
- [24] L. Li, Z. Cai, Q. Wu, W.-Y. Lo, N. Zhang, L. X. Chen, L. Yu, *J. Am. Chem. Soc.* **2016**, *138*, 7681-7686.
- [25] D. Schwarz, A. Acharjya, A. Ichangi, P. Lyu, V. Opanasenko Maksym, R. Goßler Fabian, A. F. König Tobias, J. Čejka, P. Nachtigall, A. Thomas, J. Bojdys Michael, *Chem. - Eur. J.* **2018**

COMMUNICATION

COMMUNICATION



Yaroslav S. Kochergin, Dana Schwarz, Amitava Acharjya, Arun Ichangi, Ranjit Kulkarni, Pavla Eliášová, Jaroslav Vacek, Johannes Schmidt, Arne Thomas and Michael J. Bojdys*

Page No. – Page No.

Exploring the “Goldilocks Zone” of Semiconducting Polymer Photocatalysts via Donor-Acceptor Interactions

A library of eight highly modular, photoactive S- and N- containing porous polymers (SNPs) enables us to explore the ideal conditions for photocatalytic water splitting. Intrinsic push-pull effects lead to enhanced separation of photo-induced charge-carriers and to exquisite control of the bandgap, yielding materials with highest hitherto reported hydrogen evolution rate.

Accepted Manuscript